SFDI

Daniel Molenhuis

July 2018

1 Introduction

Code snippets are contained within this writeup as well as an explanation for its use.

This is an illustration of Spatial Frequency Domain Imaging. The idea is to be able to get the vasculature targeting chlorin e6 photosensitizer to fluoresce at a wavelength of 635nm. This is a protocol aimed at treating the vasculature as a mop-up following treatment of the tumor core, penumbra, and suctioning of the large pool of blood that follows initial treatment of glioblastoma multiforme.

WHY SFDI?

This is a planar modality that mixes coherent and diffuse optical techniques for wide-field spatial localization of spectrocopic scattering of treatment drug in cancerous tissue. Retaining the pathlength information content from which a photon either is absorbed or multiply scatters is often lost with common optical methods such as: optical coherence tomography and diffuse optical tomography. SFDI is capable of quantitatively resolving the absorption and scattering by using patterned light (herein referred to as sine waves) depicted as sine waves with varying frequencies and evenly distributed phase separations (0, 120, and 240 degrees). The maximum depth at which the information content can be recovered is 8-10mm. As such, biopsied tissue can be studied at thicknesses equivalent to magnetic resonance imaging slices. The goal of which is to determine the degree of drug extravasation and the possibility of extracting mass transport coefficients in various murine brain cancer models.

SFDI is comprised of four components: Demodulation, Diffuse Reflectance Measurement, Model Inversion, and Chromophore mapping.

1. Demodulation Forward Modeling
This is a process of obtaining the envelope of the harmonically varying sine waves. A series of 7 spatial frequencies are projected as a function of wavelength. When light is projected onto the sample, the light yields a concentration of reflected light at a certain intensity with the same frequency and phase.

The change in amplitude of the sine waves is purported to contain the optical properties of the specima. We begin this measurement through demodulation. This is the quadrature of the 3 phase separations, which is capable of removing noise and ambient light. Any hint of vertical patterns remaining or if there are multiple harmonics following demodulation is an indication that the imaging session needs to be repeated. Check the Fourier transform of each of the demodulated slices of your data. Calibration to correct for non-uniformity in the instrument is necessary. This accomplished using a Spectralon commercial phantom. This will require a separate spectroscopy technique to measure the true optical properties. Furthermore a forward model is required to predict the phantom's reflectance. The model is a function of spatial frequency using the radiation transport equation solved either using the diffusion approximation or using Monte Carlo simulations.

Diffusion Approximation
A derivation of this analytical method is contained within the appendix. Of note is the dependence on the ratio of effective attenuation and transport coefficients as well as reduced albedo. At a superficial depth, the transport coefficient is the source of contrast in the sample and is largely comprised of multiple scattering events. At deeper depths, absorption is dominant. An adequate range of spatial frequencies are required wherein high spatial frequencies attenuate superficially while low spatial frequencies probe at deeper depths. There is a frequency dependence that can then be used to differentiate absorption from scattering.

Monte Carlo Simulations
The diffusion approximation is experimentally inconsistent at superficial depths. There has been a desire to compare Monte Carlo simulation to determine if improvements superficially can be made. A Monte Carlo method employed by Kienle revealed that different scattering coefficients scale photon interaction distance. This can be coupled with Beer's law:

$$R(\rho) = (\frac{\mu_s}{\mu_{s,ref}})^3 \sum_{\tau} R_{s,ref}(\rho,\tau) exp(-\mu_a v\tau)\Delta\tau \tag{1}$$

where ρ is the distance between the lense and the source, τ is the transit time, v is the speed of light, μ_s is the scattering coefficient, μ_a is the absorption coefficient, and R are the reflectance curves measured at specific wavelengths and spatial frequencies. Reflectance curves are given by a Hankel transform of zeroth order:

$$R(k_x) = 2\pi \sum_{i=1}^{n_p} \rho_i J_0(k_x,\rho_i) R(\rho_i) d\rho_i) \tag{2}$$

where J_0 is a Bessel function of the first kind and n_p are the step sizes of the radial distance of τ. The above equation is used to generate a mesh of 7 spatial frequencies for a series of absorption and scattering coefficients. A minimization scheme is used to fit measured relative to simulated optical properties.

Obtaining Optical Properties

Apart from the minimization scheme to tease out absorption and scattering coefficients, spectral parameters are also required. The spectral parameters are the scattering amplitude (α) and slope of the scatterers (β) as well as concentration of tissue chromophores given *a priori* extinction coefficients of likely chromorphores in the sample such as oxygenated blood (HbO_2), deoxygenated blood (Hb), and water ($H2O$).

Dimensional Analysis

A power law dependence describes Mie scattering making it a function of the density and size of chromophores whose scattering amplitude (α) and power (β) coefficients are given by:

$$\alpha = \frac{\sum_\lambda ln\mu_s(\lambda_0) - \beta \sum_\lambda ln(\frac{\lambda}{\lambda_0})}{n} \tag{3}$$

$$\beta = -\frac{n\sum_\lambda ln(\frac{\lambda}{\lambda_0}) ln\mu_s(\lambda_0) - \sum_\lambda ln(\frac{\lambda}{\lambda_0}) \sum_\lambda ln\mu_s(\lambda_0)}{n\sum_\lambda ln(\frac{\lambda}{\lambda_0})^2 - (\sum_\lambda ln(\frac{\lambda}{\lambda_0}))^2} \tag{4}$$

where n are all the wavelengths used in your measurements.

This gives us a scattering model:

$$\mu_s(\lambda) = \alpha\mu_s(\lambda_0)(\frac{\lambda}{\lambda_0})^{-\beta} \tag{5}$$

Absorption coefficients are derived from known concentrations and extinction spectra of HbO_2, Hb, $H2O$. Other chromophore concentrations need to be confirmed from pathology and are pending. This will reveal important characteristics such as $TGF-\beta$, fat content, hypoxia, mean vessel density, and mean vessel area.

Data Mining

Supervised (k-nearest neighbour (knn)) and unsupervised (independent components analysis (ICA)) machine learning was deployed to automate the differentiation between brain pathologies and chromorphores per pixel. kNN parametrically assigned to a 5-D vector with non-overlapping sets and cross validation using receiver operator characteristics.

I am working with an aggressive brain cancer model. Here is a visualization of the brain with the drug injected intravenously prior and imaged with

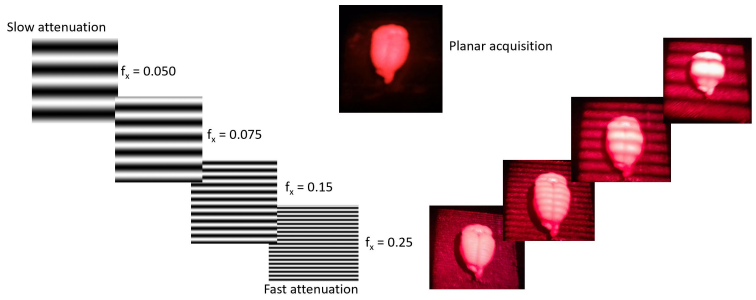

Figure 1: MTFs at different frequencies

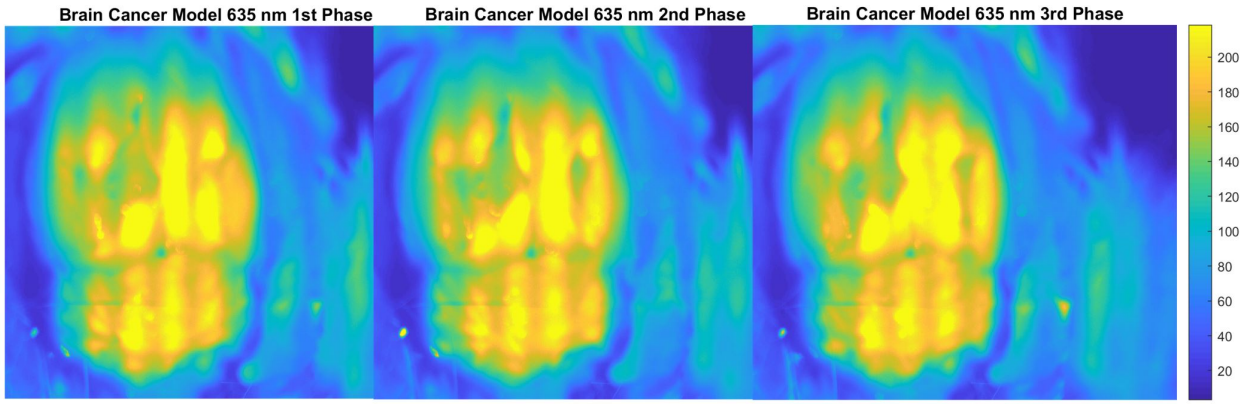

Figure 2: 3 phase technique: 0 degrees, 120 degrees, 240 degrees

15 MTFs (typically use a range of 7 to 14 plus an image sequence without the MTFs). Figure 1 is just an idea of what the MTF projections look like and their subsequent display on tissue. We also need to display these patterns on phantoms, which will be described in the second part of this tutorial.

After observing the MTF at the three phase shifts (Figure 2), obtain the pixel dimension of your field of view (Figure 3). Next we obtain the Fourier Transform of each image (cannot be automated) using a line profile, which may be quite tedious but important.

The fundamental is at 7 cycles per row (Figure 4 below).

As we peruse other MTF datasets, harmonics may be observed (Figure 5). Note the second harmonic at 11 cycles/row. We may see artifacts in our demod-

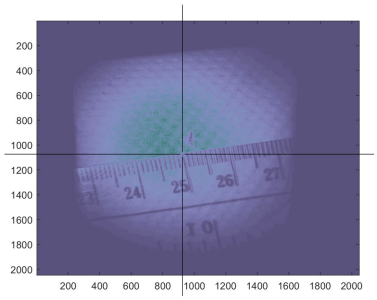

Figure 3: Determining pixel dimension

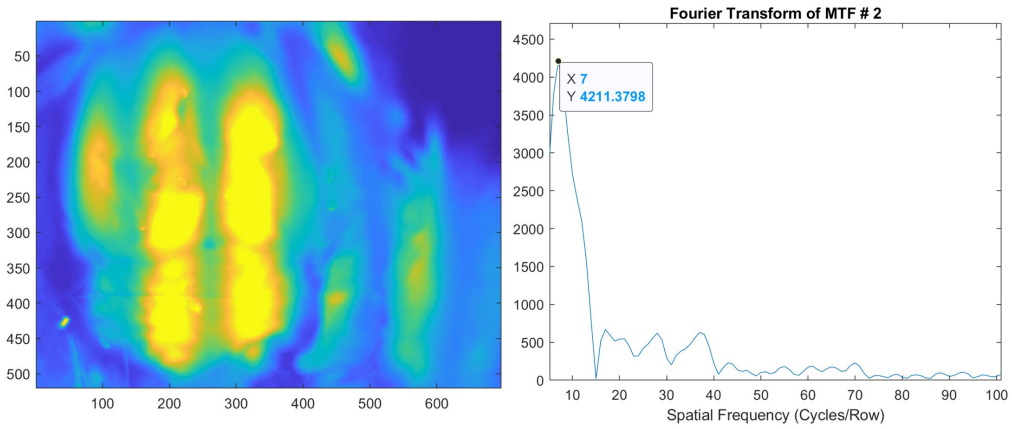

Figure 4: Fourier Transform of MTF at 0.05/mm. Fundamental at 7.

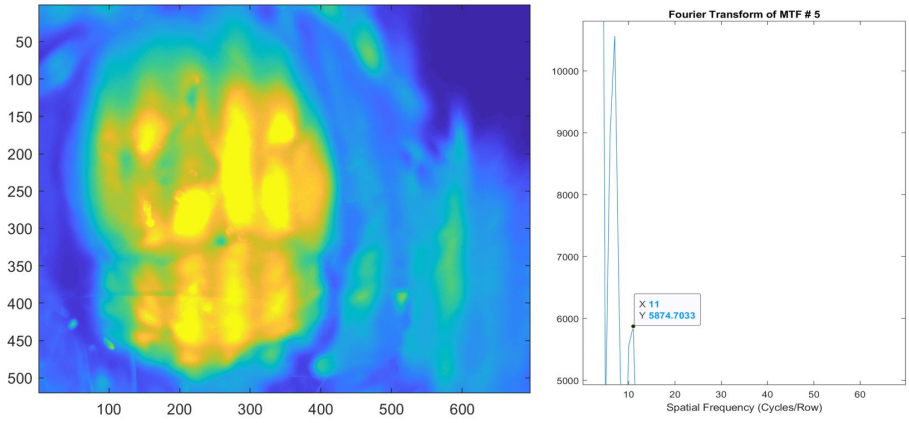

Figure 5: Fourier Transform of MTF at 0.075/mm. Second harmonic at 11.

ulation as a consequence and will have to re-measure our sample or discard the measurement entirely. In figure 6 we do not see any vertical deviations although an error metric should be considered which is displayed in Figure 7. We see that the largest variance occurs at the 8th MTF pattern.

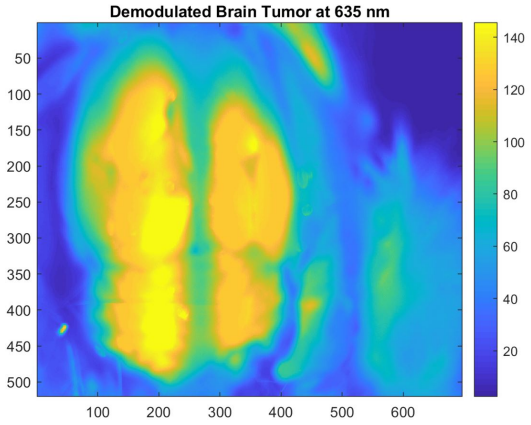

Figure 6: Demodulation of MTF at 0.05/mm

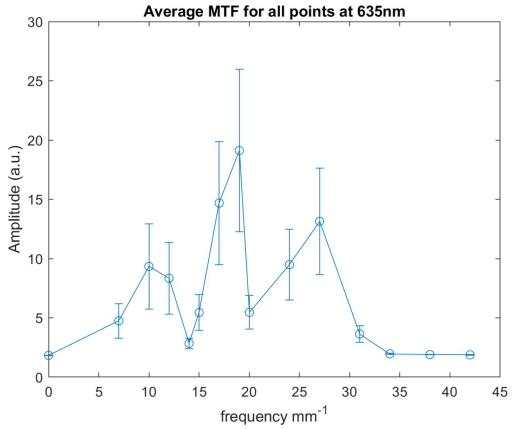

Figure 7: The largest standard deviation appears between 16 to 19/mm